16TH EUROPEAN CONFERENCE ON EARTHQUAKE ENGINEERING THESSALONIKI 18 - 21 JUNE 2018

INTEGRATION OF SITE EFFECTS INTO PSHA: A COMPARISON BETWEEN TWO FULLY PROBABILISTIC METHODS FOR THE EUROSEISTEST CASE.

Claudia ARISTIZÁBAL[1], Pierre-Yves BARD[2], Juan Camilo GÓMEZ[3] Céline BEAUVAL[4]

ABSTRACT

Several approaches have been proposed to integrate site effects in Probabilistic Seismic Hazard Assessment (PSHA), varying from deterministic, to hybrid (probabilistic-deterministic), and finally fully probabilistic approaches. The present study compares hazard curves obtained for a soft, non-linear site with two different, fully probabilistic site specific seismic hazard methods: 1) The Full Convolution Analytical Method (AM) (Bazzurro and Cornell 2004a,b) and 2) what we call the Full Probabilistic Stochastic Method (SM). The AM computes the site-specific hazard by convolving the site-specific bedrock hazard curve, Sar(*f*), with a simplified representation of the probability distribution of the amplification function, AF(*f*) at the considered site, while the SM is built from stochastic time histories on soil corresponding to a representative, long enough catalogue of seismic events. This comparison is performed for the example case of the Euroseistest site near Thessaloniki (Greece). We generate a hazard-consistent synthetic earthquake catalogue, apply host-to-target corrections, calculate synthetic time histories with the stochastic point source approach, and scale them using an adhoc frequency dependent correction factor to fit the specific rock target hazard. We then propagate the rock stochastic time histories, from depth to surface using two different 1D site response analysis, a linear equivalent (LE) and non-linear (NL) codes, to evaluate the code-to-code variability. Lastly, we compute the probability distribution of the non-linear site amplification function, AF(*f*), for both site response approaches, and derive the site-specific hazard curve with both AM and SM approaches. Results are found in relatively satisfactory agreement whatever the site response code along all the studied periods. The code-to-code variability (EL and NL) is found significant, providing a much larger contribution to the hazard estimate uncertainty, than the method-to-method variability (AM and SM). However, the AM approach presents a numerical limitation, that is not encountered with the SM approach, though with a much higher computational price. The use of stochastic simulations to integrate site effects into PSHA allows to better investigate the variability of the site response physics, and a good parameterization of the input parameters, something that currently is not possible with real data due to its scarcity especially at high acceleration levels.

Keywords: Site Response; PSHA; Non-linear behavior; Host-to-target adjustment; stochastic simulation.

1 INTRODUCTION

The integration of site effects into Probabilistic Seismic Hazard Assessment (PSHA) is a constant subject of discussion within the seismic hazard community due to its high impact on hazard estimates. A relevant overview and enlightening examples can be found for instance in Bazzurro and Cornell 2004a,b and Papaspiliou et al. 2012a,b. However, it is still treated in a rather crude way in most engineering studies, and the variability associated to the non-linear behavior of soft soils is not fully or not properly taken into account. For instance, all the various approaches discussed in Aristizábal et al. (2017, 2018a) to include site effects into PSHA correspond to hybrid (deterministic – probabilistic) approaches, for which the (probabilistic) uniform hazard spectrum S_{ar} on the specific bed rock of a given site is simply multiplied by the median site-specific amplification function AF(*f; S_{ar}*), possibly

[1] PhD candidate, ISTerre, U. Grenoble Alpes, Grenoble, France, claudia.aristizabal@univ-grenoble-alpes.fr
[2] Researcher, ISTerre, U. Grenoble Alpes/CNRS/IFSTTAR, France, pierre-yves.bard@univ-grenoble-alpes.fr
[3] MEEES Master student, ISTerre, U. Grenoble Alpes, Grenoble, France, jcgomezz1910@gmail.com.
[4] Researcher, ISTerre, U. Grenoble Alpes /CNRS/IRD, France, celine.beauval@univ-grenoble-alpes.fr

including non-linear site response for this particular ground motion level. The main drawback of those different hybrid-based approaches is that once the hazard curve on rock is convolved with the local non-linear, frequency dependent amplification function, AF($f;S_{ar}$), the exceedance probability at site surface is no longer the one defined initially for the bedrock hazard: at a given frequency, the same surface ground motion can be reached with different reference bedrock motion (corresponding to different return periods and/or different scenario earthquakes) and different non-linear site response. This issue was investigated by Bazurro and Cornell 2004b, who concluded for their two example sites (clay and sand), that the hybrid-based method tends to be non-conservative at all frequencies and at all mean return periods with respect to their approximation of the fully probabilistic method. The present work constitutes a further step along the same direction, trying to overcome the limitation of hybrid-based approaches for strongly non-linear sites by providing a fully probabilistic description of the site-specific hazard curve. It presents a comparison exercise between hazard curves obtained with two different, fully probabilistic site-specific seismic hazard approaches: 1) The Full Convolution Analytical Method (AM) proposed by Bazurro and Cornell 2004a and 2) what we call the Full Probabilistic Stochastic Method (SM). The AM computes the site-specific hazard on soil by convolving the site-specific hazard curve at the bedrock level, $S_{ar}(f)$, with a simplified representation of the probability distribution of the site-specific amplification function, AF(f; S_{ar}), while the SM derives hazard curves directly from a large set of synthetic time histories at site surface, combining simple point-source stochastic simulations for bedrock on a hazard-consistent event catalogue, and non-linear site response for all bedrock time histories. This comparative exercise is implemented here for the Euroseistest site, a multidisciplinary European experimental site for integrated studies in earthquake engineering, engineering seismology, seismology and soil dynamics (Pitilakis et al. 2013).

2 STUDY AREA: THE EUROSEISTEST SITE

As stated in Pitilakis et al. 2013, *"the Euroseistest site is a multidisciplinary European experimental site for integrated studies in earthquake engineering, engineering seismology, seismology and soil dynamics. It is the longest running valley-instrumentation project worldwide, and is located in Mygdonia valley (epicenter area of the 1978, M6.4 earthquake), about 30 km to the NE of the city of Thessaloniki in northern Greece. It consists of a 3D strong-motion array and an instrumented SDOF structure (EuroProteas) to perform free and forced tests"* (see **Figure 1**). This site was selected as an appropriate site to perform this exercise, because of the availability of extensive geological, geotechnical and seismological surveys. The velocity model of the Euroseistest basin has been investigated by several authors (Jongmans et al. 1998; Raptakis et al. 2000; Chávez-García et al. 2000), and was used to define 1D soil column for the present exercise (**Figure 2a** and **Table 1**).

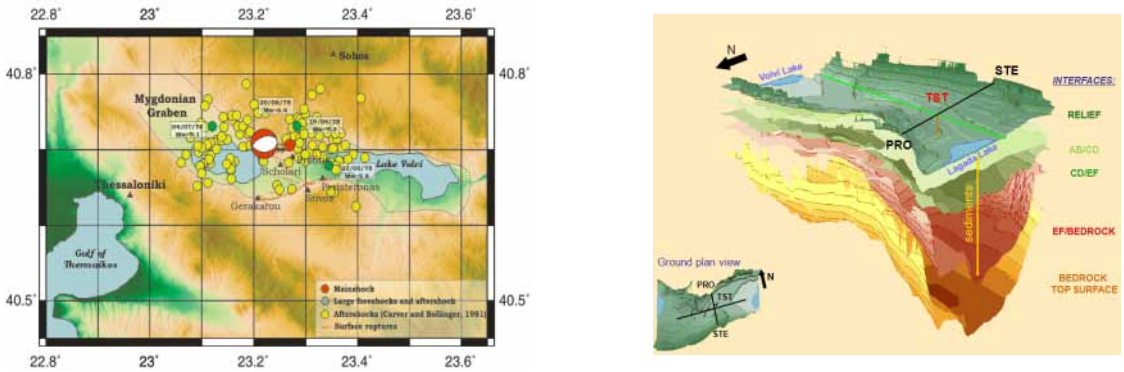

Figure 1. (a) Map showing the broader region of occurrence of the 20 June 1978 (M6.5) earthquake sequence. Epicenter and focal mechanism (Liotier 1989) of the mainshock (red) and epicenters of the largest events of the sequence (green, yellow) (Carver and Bollinger, 1981) are indicated (from http://euroseisdb.civil.auth.gr/geotec). **(b)** 3D model of the Mygdonia basin geological structure (Manakou et al., 2010).

Degradation curves are also available to characterize each soil layer, (**Figure 2b,c**), (Raptakis et al., 1998) and local recordings as well to calibrate the model in the linear (weak motion) domain. Several studies performed at the Euroseistest, both instrumental and numerical, have consistently shown a

fundamental frequency (f_0) around 0.6 - 0.7 Hz (Riepl et al., 1998, Raptakis et al., 2000, Maufroy et al., 2015, 2016 and 2017) with an average shear wave velocity over the top 30 meters V_{S30} equal to 186 m/s. The 1D simulations performed in this study are based on the parameters listed in **Table 1**, which have been shown to be consistent with the observed instrumental amplification functions, AF(*f*), at least in the linear domain.

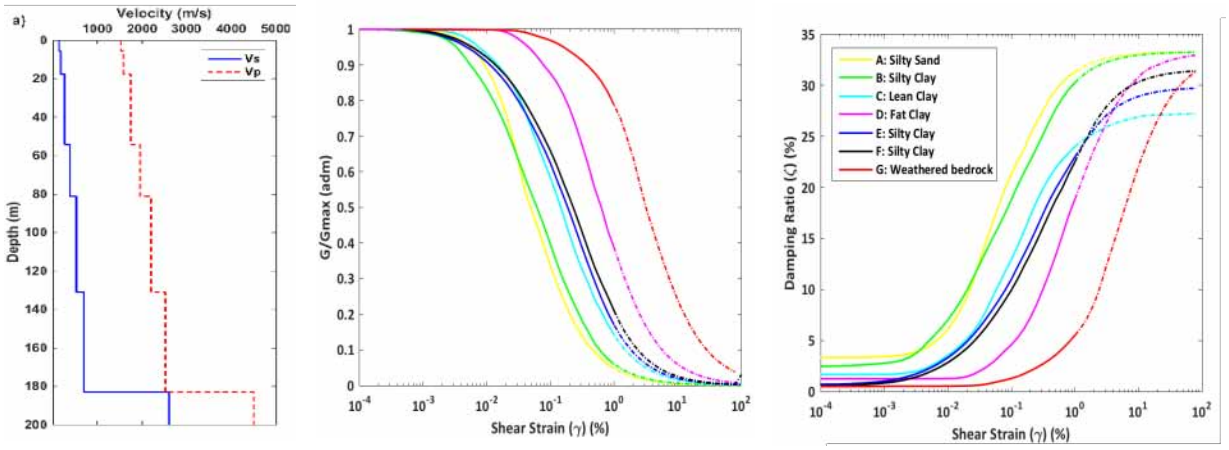

(**a**) (**b**) (**c**)

Figure 2. (a) 1D shear wave, Vs, and compressive wave velocity, Vp, velocity profiles between TST0 and TST196 stations, located at the middle of the Euroseistest basin, at surface and 196 m depth, respectively. Euroseistest shear modulus **(b)** and damping ratio **(c)** degradation curves (Pitilakis et al., 1999).

Table 1. Material properties of the Euroseistest soil profile used for the site response calculations.

Layer	Depth (m)	Vs (m/s)	Vp (m/s)	ρ (kg/m^3)	Q	ϕ'	Ko'
1	0.0	144	1524	2077	14.4	47	0.26
2	5.5	177	1583	2083	17.7	19	0.67
3	17.6	264	1741	2097	26.4	19	0.68
4	54.2	388	1952	2117	38.8	27	0.54
5	81.2	526	2200	2151	52.6	42	0.33
6	131.1	701	2520	2215	70.1	69	0.07
7	183.0	2600	4500	2446	-	-	-

*Water table at 1 m depth. Vs: shear wave velocity. Vp: Compressive wave velocity. ρ : soil density. Q: Anelastic attenuation factor. φ: Friction angle. Ko: Coefficient of earth at rest.

3 METHODOLOGY

The methods followed in this work correspond to two different, fully probabilistic procedures to account for highly non-linear soil response in PSHA, a Full Probabilistic Stochastic Method (SM) developed for the present work, and the Full Convolution Analytical Method (AM).
For both approaches, the first step is to derive the hazard curve for the specific bedrock properties of the considered site. As shown in **Table 1** and **Figure 2**, this bedrock is characterized by a large S-wave velocity (2600 m/s), and is therefore much harder than "standard rock" conditions corresponding to V_{S30} = 800 m/s. This step must thus include host-to-target corrections ("HTT", Cotton et al. 2006; Van Houtte et al. 2011; Delavaud et al., 2012; Biro and Renault 2012). For sake of simplicity in the present exercise, the hazard curve has been derived with only one GMPE (Akkar et al., 2014), which is satisfactorily representative of the mean hazard curve obtained with seven other GMPEs deemed relevant for the European area. For sake of simplicity also, the HTT adjustments have been performed on the basis of simple velocity adjustments calibrated on KiKnet data (Laurendeau et al., 2017).

For the SM approach, the next step consists in generating a synthetic earthquake catalog sampling the magnitude-frequency distribution (better known as the Guttenberg-Richter Law) of the area source zone of the SHARE Seismotectonic model (Woessner et al. 2015, Pagani et al. 2014). This synthetic

earthquake catalog was derived using the Stochastic Event Set Calculator tool of the OpenQuake engine (Pagani et al. 2014), and is characterized by a set of events with magnitude-distance (M,D) couples corresponding to a total duration of 50000 years. It was then used to generate compatible synthetic time histories on rock using the Boore 2003 Stochastic Method (Boore 2003, 2005). By compatible we mean that the hazard curve on rock generated with the classical PSHA method, is (approximately) equal to the hazard curve built from the generated stochastic time histories. This component of the approach is not trivial however, and requires specific adjustments / corrections that are described in the results section. All such hard rock corrected and scaled time histories are then propagated from depth to surface using two different 1D non-linear site response codes, in order to obtain a large set of surface time histories corresponding to the whole catalogue of seismic events representative of the site hazard. One set of time histories on soil is based on the SHAKE91 (Schnabel 1972; Idriss and Sun 1993; Schnabel et al. 2001) linear-equivalent code (LE), while the second set was derived using the NOAH (Bonilla 2001), fully non-linear code (NL). Both codes were used with the aim to get a hint of the code-to-code variability. The next and final SM step consists in deriving the site-specific hazard curve by simply calculating the annual rate of exceedance of all surface synthetics.

The AM approach requires to describe the amplification function AF(f; S_{ar}) and its variability as a function of frequency and input motion level and waveform, with a piecewise linear function with appropriate lognormal distribution, for both site response analysis codes (LE and NL). The large number of computations required by the SM approach were also used to derive this simplified representation of amplification factors. The bedrock hazard curve (including HTT adjustments) could then be convolved analytically with this simplified decscription of amplification factor using the mathematical framework developed by Bazzurro and Cornell (2004b), to obtain another estimate of the site surface hazard curve, to be compared with the SM estimate.

4 RESULTS

The site-specific soil hazard estimates at the Euroseistest using the two different fully probabilistic methods are presented below, after presentation of the intermediate step results obtained with the described methodology and with some discussion on the various required assumptions.

4.1 Rock Target Hazard

The first step consists in defining the target hazard on "standard rock" at the Euroseistest. This was done with the Akkar et al. 2014 GMPE for V_{S30} = 800 m/s, the Openquake Engine (Pagani et al. 2014) and the seismotectonic model proposed on the European SHARE project (Woessner et al. 2015). The resulting hazard curves are displayed in **Figure 3** for the spectral acceleration at three different periods (0, 0.2 and 1.0 s, respectively)

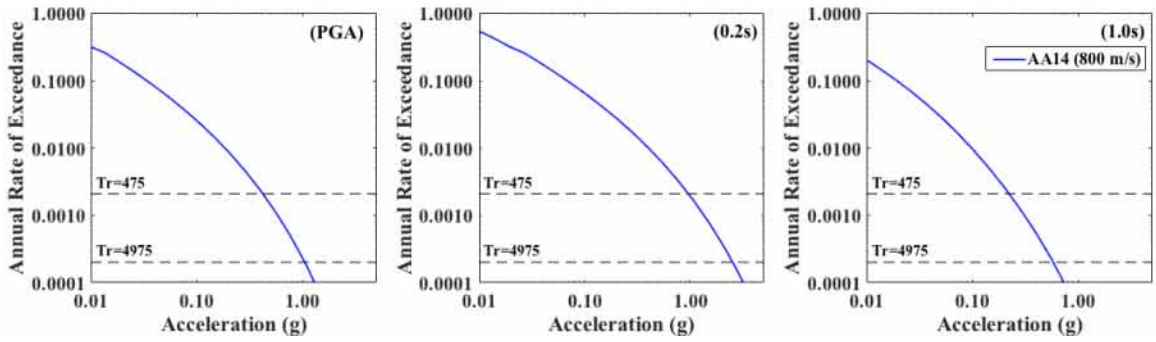

Figure 3. Target hazard curve on rock (Vs=800 m/s) at the Euroseistest calculated using the Akkar et al., 2014 GMPE (AA14) for three different spectral periods (PGA, 0.2s, 1.0s).

4.2 Synthetic Earthquake Catalog

Once defined the target hazard on standard rock, we proceed to generate a hazard consistent stochastic

seismic catalogue, comprising enough seismic events to build synthetic hazard curves for standard rock at the selected site. This was done again with the Openquake Engine (Pagani et al. 2014). A sensitivity analysis regarding the respective contributions to the total hazard of the various area sources surrounding the Euroseistest according to the SHARE seismotectonic model, indicated that for the considered return periods, the rock hazard is almost fully controlled by one single crustal area source, i.e., the "GRAS390" one containing the Euroseistest site. The stochastic earthquake catalog was thus generated with the Stochastic Event Set Calculator tool implemented in the Openquake Engine, after sampling the frequency-magnitude distribution (i.e., the Gutenberg-Richter law) of the GRAS390 crustal area source zone. The associated Monte Carlo simulation approach results in homogeneously distributed earthquakes inside the selected source zone. A sensitivity analysis on the catalogue length (considering 500, 5.000, 25.000, 35.500 and 50.000 years) showed that only the catalogue length of 50.000 years allows replicating the target rock hazard curve with an acceptable level of misfit (<5%) for all oscillator periods up to a return period of 5.000 years. The final, so selected catalogue consists of a total of 21806 events ranging from the minimum considered magnitude (4.5) to 7.8, in a distance range from 0 to 150 km, and a depth range from 0 to 20 km.

4.3 Host-to-target Adjustments

As discussed in more detail in Aristizábal et al. (2017, 2018a), the bedrock underneath the Euroseistest basin (~196 m depth) has a shear wave velocity of about 2600 m/s, much larger than the useable ranges of almost all GMPEs. It is therefore mandatory to perform "host-to- target adjustments" (HTTA) corrections (Cotton et al. 2006; Van Houtte et al. 2011; Delavaud et al. 2012; Biro and Renault 2012). This type of host-to-target corrections is extensively discussed in Aristizábal et al. (2017, 2018a). However, the high level of associated uncertainty, and the questions recently raised about the reliability of usual V_{S30}-κ_0 relationships (Ktenidou and Abrahamson, 2016; Kottke, 2017; Laurendeau et al., 2017), together with the significant level of complexity and subjectivity involved in the current HTTA procedures (Campbell, 2003; Al Atik et al., 2014), led us to use in this paper another, much simpler and straightforward, way to account for rock to hard rock correction for probabilistic seismic hazard purposes.

This new way is based on the recent work by Laurendeau et al. 2017, who proposed rock GMPEs valid for surface velocities ranging from 500 m/s to 3000 m/s, on the basis of a KiK-net subset. These GMPEs present the double advantage to rely only on the value of rock velocity, without needing the κ_0 values neither for the host region nor for the target site, and provide rather robust predictions of rock motion whatever the approach used for their derivation (deconvolution of surface recordings to outcropping bedrock with the known 1D profile, or correction of down-hole recordings). The "LA17" GMPE used in the following LA17 is based on a combined data set including surface recordings from stiff sites and hard rock motion estimated through deconvolution of the same recordings by the corresponding 1D linear site response. The site term in the corresponding (simple) GMPE equation is given by a simple dependence on rock S-wave velocity value V_{S30} in the form $s_1(T).\ln(V_{S30}/1000)$, where s_1 is tuned from actual recordings for each spectral oscillator period T. The HTT adjustment factor can thus be computed as follows:

$$HTT\ Adjustment\ Factors = \frac{LA17\ HC\ Hard\ Rock\ (Vs = 2600\ m/s)}{LA17\ HC\ Standard\ Rock\ (Vs = 800\ m/s)} = s(T).ln(2600/800) \qquad (1)$$

Since the site terms in LA17, for such hard and standard rock, do not include any non-linearity, the resulting HTT adjustment actors are ground-motion independent, and thus return period independent. The values listed in Table 2 indicate that hard rock motion is systematically smaller than the standard rock motion at all spectral periods, with larger reduction factors at short periods. Of course these corrections are in principle valid only for Japanese rock sites, but most of HTTA methods are implicitly based on US / California type of rocks, which are often applied to many other parts of the world without special warning.

Ultimately, the hard rock hazard curve is then derived by simply scaling the AA14 hazard curve with

the HTTA factors for each period (Figure 4). One might wonder why scaling AA14 curve instead of using directly LA17 in the calculations. The main reason was that AA14 (Vs=800 m/s) provide a good approximation to the mean hazard estimate at the Euroseistest on standard rock from seven explored GMPES (Aristizábal et al. 2018a), while the estimates with LA17 (Vs=800 m/s) is located outside the uncertainty range of the same selected representative GMPEs: this is probably due to the very simple functional form used in LA17, and to the fact it is elaborated only from Japanese data. Its main interest however is to provide a rock adjustment factor calibrated on actual data from a large number of rock and hard rock sites, without any assumptions regarding non-measured parameters such as κ_0. Once the approach proposed in Laurendeau et al. (2017) will be applied to other data sets, the corresponding results can be used to provide alternative scaling factors between hard rock and standard rock.

Table 2 : Host-to-target adjustments factors derived using LA17 hazard curves from a standard rock (VS30=800 m/s) to the Euroseistest hard rock (VS30=2600 m/s).

Spectral Period (s)	**PGA**	**0.05**	**0.1**	**0.2**	**0.5**	**1.0**	**2.0**
HTT adjustment factor	0.47	0.45	0.38	0.51	0.70	0.78	0.86

4.4 Synthetic Time Histories on Rock

The previously derived earthquake catalogue is then used to generate hazard consistent synthetic time histories on hard rock with the well known Ground-motion Simulation Stochastic Method (Boore 2003), as implemented in the corresponding Fortran code SMSIM (Boore 2005). The selection of this code for the generation of synthetic time histories was our particular choice, however, any other suitable method to generate synthetic time histories is also suitable. This step is undoubtedly one of the most time consuming of the entire process, since the large return periods considered here require to perform such simulations for a very large number (~21800) of events. The main input parameters for the Boore stochastic method (Boore 2003) are the moment magnitude (M_W), the distance (D_{hyp}), the stress drop ($\Delta\sigma$), the crustal amplification factor (CAF(f)), and the high frequency site attenuation factor, Kappa (κ_0). Considering the published, locally available data at the Euroseistest, the Boore stochastic method has been applied wit the crustal velocity structure detailed in Maufroy et al. 2017, a κ_0 value of 0.024s (Ktenidou et al., 2015; Perron et al. 2016) and a lognormal distribution of the stress drop with a mean value of 30 bars and an associated standard deviation of 0.68. The resulting raw hazard curves are displayed in red on Figure 4.

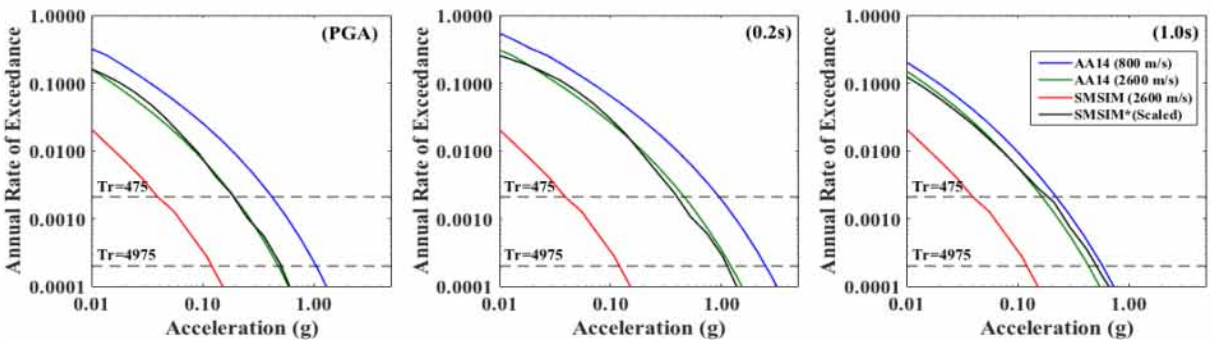

Figure 4. Hazard curves for three different spectral periods (PGA, 0.2s, 1.0s): AA14 (800 m/s) HC on standard rock (blue). AA14 (2600 m/s) HC on hard rock after HTT (green). SMSIM (2600 m/s) HC built from synthetic time histories on hard rock, 2600 m/s, using Boore 2003 stochastic method (red). SMSIM (Scaled) is the HC built from synthetic time histories on hard rock, SMSIM (2600 m/s), and scaled to match AA14 (2600 m/s) HC.

They are found not to fit the target hard-rock hazard curve (green curves in Figure 4). Such a discrepancy is related to the lack of consistency between the theoretical, stochastic approach and the empirical AA14 GMPE; it was thus corrected by applying frequency dependent scaling factors derived from the ratios between SMSIM and AA14 hazard curves for a target hard-rock velocity of 2600 m/s. These scaling factors were applied on the Fourier spectra of the stochastic time series and a set of 21

806 modified hard-rock, synthetic time series were obtained by inverse Fourier transform. The distribution of the resulting response spectra values for the set of modified synthetics allowed deriving the scaled hazard curves displayed in black on Figure 4. This scaling allowed to obtain a very satisfactory fit of the target AA14 hazard curve for a 2600 m/s hard-rock site at the three different spectral periods, a task that is not possible to perform by common, time domain scaling techniques.

4.5 Non-Linear Site Response and resulting hazard curves

This set of ~21800 modified time histories was then considered as the outcropping hard-rock motion and propagated through the 1D soil column described in **Figure 2** and **Table 1** to obtain a corresponding series of ~21800 site surface motion synthetics. Two site response analysis approaches were considered, the SHAKE91 1D linear equivalent (LE) code (Schnabel et al., 1992) and the NOAH 1D non-linear (NL) code (Bonilla, 2001), respectively. The corresponding amplification factors for pga are displayed in **Figure 5**. These two sets of site surface synthetics were then used to derive the site-specific hazard curves in two different ways, SM and AM.

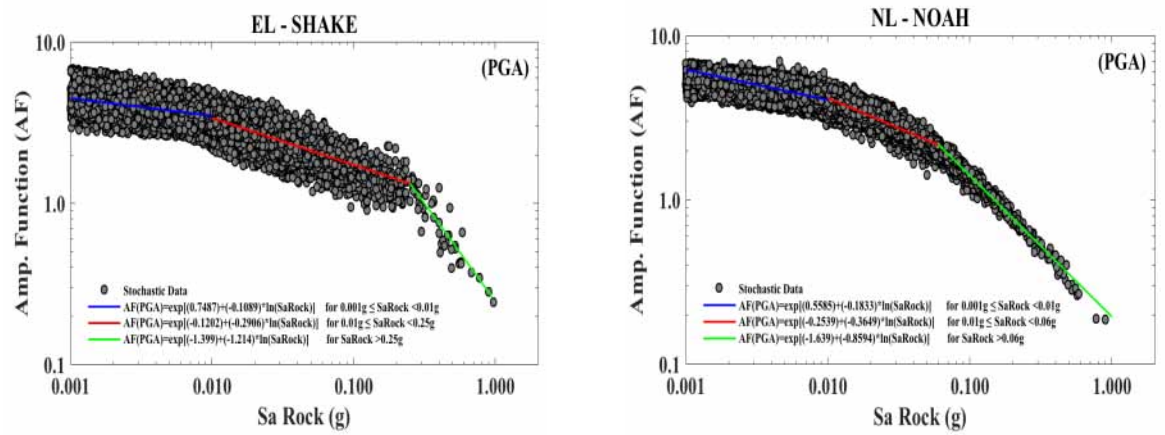

Figure 5. Amplification factors for pga as a function of rock pga as derived with EL-SHAKE91 (left, a) and NK-NOAH (right, b) site response computations for the set of 21806 rock synthetics. Each plot also displays a tri-linear piecewise regression models of $AF(f)$ on $S_{ar}(f)$ f.

4.5.1 Full Probabilistic Stochastic Method (SM)

What it is called here the Full Probabilistic Stochastic Method, SM, is nothing else than the hazard curve built directly from the set of synthetic time histories at site surface. The annual rate of exceedance of a certain ground-motion level (X), is obtained by counting the number of events for which the considered ground motion parameter x is exceeding the X value, and dividing it by the catalogue length as expressed in Eq. (2).

$$\lambda(x \geq X) = \frac{N_{events}\ (x \geq X)}{Catalogue\ \ time\ length} \qquad (2)$$

The resulting hazard curves at site surface are displayed in **Figure 6** for three different spectral periods (PGA, 0.2s and 1.0s), for LE (SHAKE91, red solid line) and NL (NOAH, green solid line) site response computations.

4.5.2 Full Convolution Analytical Method (AM)

In order to obtain fully probabilistic, site-specific hazard curves, Bazurro and Cornell (2004a,b) proposed three different approaches based on convolving the bedrock specific hazard curve with more or less simple descriptions of the site amplification function, AF(*f*, *Sar*). These approaches are intended to provide more precise and reliable surface ground-motion hazard estimates than those found by means of standard attenuation laws for generic soil conditions. One of the proposed methods

is called "Analytical Estimate of the soil hazard" corresponds to the Full Convolution Analytical Method (AM) or as they. It is based on a piecewise linear representation of the site amplification function AF(*f*, *Sar*) = C_0 + C_1 ln(S_{ar}(f)) with a lognormal standard deviation $\sigma_{\ln(AF(f))}$ (see **Figure 5**), from which a simple, closed-form solution is obtained that appropriately modifies the hazard results at the rock level, to finally obtain the hazard curve on soil, Eq. (3).

$$HC_{Soil}(f) = HC_{Rock}(f)\ .\ e^{\left(\frac{1\ {k_1}^2\sigma^2}{2(C_1+1)^2}\right)} \qquad (3)$$

Where C_1 and $\sigma_{\ln(AF(f))}$ are the slope and standard deviation of the piecewise-linear regression models of the AF(*f*) vs. S_{ar}(*f*) as proposed by Bazurro and Cornell 2004b (and shown in **Figure 5** for the present example), and k_1 is the slope (in log–log scale) of the straight-line tangent to the rock hazard curve at the point, thus corresponding to the exponent of the local power law representation of the bedrock hazard curve, i.e., HC [S_{ar}(f)] = $K_0.S_{ar}(f)^{-k_1}$.

Table 3. Slope (C1) and standard deviation (σ) of the piecewise-linear models (PLM) of the AF(*f*) Vs. Sar(*f*).

Spectral Period (s)	Piecewise-Linear Models	SHAKE91		NOAH	
		C_1	σ[ln(AF)]	C_1	σ[ln(AF)]
PGA	PLM 1 (Blue)	-0.1089	0.15	-0.1833	0.11
	PLM 2 (Red)	-0.2906	0.19	-0.3649	0.08
	PLM 3 (Green)	-1.2140	0.19	-0.8594	0.08
(0.2)	PLM 1 (Blue)	-0.1475	0.19	-0.1020	0.12
	PLM 2 (Red)	-0.4043	0.18	-0.4789	0.13
	PLM 3 (Green)	-1.1970	0.27	-1.1172	0.35
(1.0)	PLM 1 (Blue)	-0.0561	0.27	-0.0170	0.11
	PLM 2 (Red)	-0.1438	0.14	-0.3298	0.22
	PLM 3 (Green)	-1.2900	0.08	-1.4930	0.26

The main advantages of this method are: (1) The amplification produced due to the soil site effects is considered as an a posteriori correction to the hazard calculations. (2) The full meaning of the hazard curve and UHS is respected. (3) The calculations of the hazard curve on soil are very simple and with low computational demand. (4) Fewer accelerograms are required to calculate the AF(*f*, S_{ar},) than the SM, resulting in a much lower computational demand.

The AM hazard curves at site surface were calculated in that way again for different spectral periods (PGA, 0.2s and 1.0s), and are shown also in **Figure 6** (dotted lines) The same 1D linear equivalent (LE) and 1D non-linear (NL) site response analysis as in the SM approach, using SHAKE91 and NOAH (red and green) respectively, were used to derive the piecewise linear approximations (**Table 3**) and the associated $\sigma_{\ln(AF(f))}$ values.

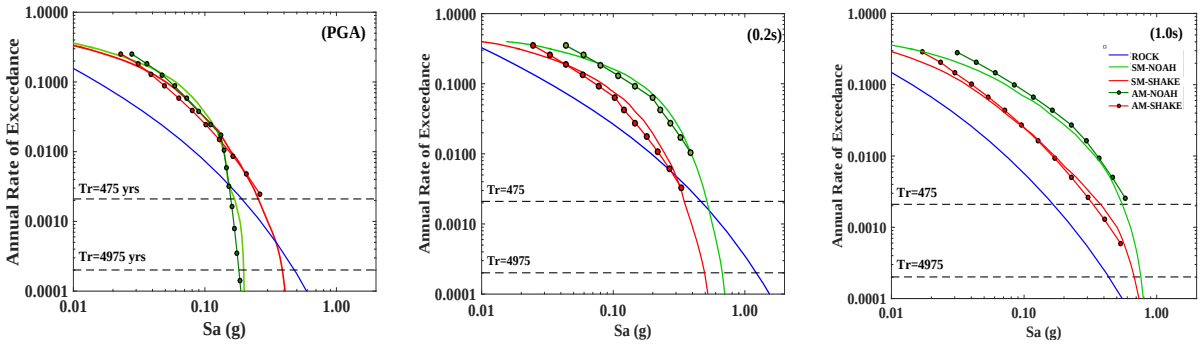

Figure 6. Median hazard curves at site surface using both equivalent-linear SHAKE91 (red) and nonlinear NOAH (green) for both AM (dotted line) and SM (continuous line) at three different spectral periods (PGA, 0.2s and 1.0s). Also shown is the hazard curve for the reference rock (2600 m/s, blue curve)

5 DISCUSSION

This comparison indicates that hazard curves calculated using the Full Convolution Analytical Method (AM) and the Fully Probabilistic Stochastic Method (SM), present a good agreement at all considered return periods and spectral periods (**Figure 6**). Nevertheless, and despite the good fit between both methods, the AM method presents an intrinsic numerical limitation that did not allow us to calculate the site surface hazard curve even at the most common, 475 years return period. This limitation is related to the values of C_1 and $\sigma_{\ln(AF(f))}$ in the modifying term of equation (3) : when C_1 is close to -1, and/or the site response variability $\sigma_{\ln(AF(f))}$ is large, the modifying site factor term may become very large, and so is the site hazard. As shown in **Figure 5**, **Table 1**, and **Figure 7**, C_1 values close to -1 may be obtained when the surface motion saturates because of strong non-linearity, and relatively large site response variability are obtained, especially at large rock motion levels and for the 1s period. This obviously raises questions about the AM effectiveness to account for non-linear site effects in PSHA. It is important though to emphasize that this limitation only affects sites with strong non-linear and/or high seismic demands such is the case in the present example. When such a limitation is faced, a possible, conservative way to cope with it could be to set a minimum value – larger than -1.0 - of the slope (C_1) of the amplification regression (AF(f) vs $S_{ar}(f)$). This would allow the exponential term related to the soil factor in Eq. (3) (Bazzurro and Cornell 2004b Eq. 17) to remain within "reasonable bounds", in order to continue using the AM at long return periods. However, it is important to keep in mind that setting such a minimum value for C_1, is equivalent to setting a upper bound to the amount of non-linearity in the site response, resulting in particular in the absence of any saturation, which is not easily acceptable from a physical viewpoint.

We can also highlight that most of the variability in terms of hazard estimates are due to the code-to-code (SHAKE91, NOAH) variability and the soil column modeling, rather than the method-to-method (AM, SM) variability. As shown in **Figure 7**, SHAKE91 tends to predict larger values of surface PGA for high bedrock input level, while the trend is opposite for the two other spectral periods (0.2s and 10.s). One may also notice a significant non-linear behavior even at low frequencies (1.0s), and relatively low return periods, which is related to the facts that such a period is already shorter than the site fundamental period (around 1.4 s), and that the velocity contrast at the sediment-bedrock interface is quite large (see **Table 1**): this induces large strains at large depth, which in turn impacts the shear modulus and damping values over the whole soil column, and significantly decreases the amplification and thus the surface motion.

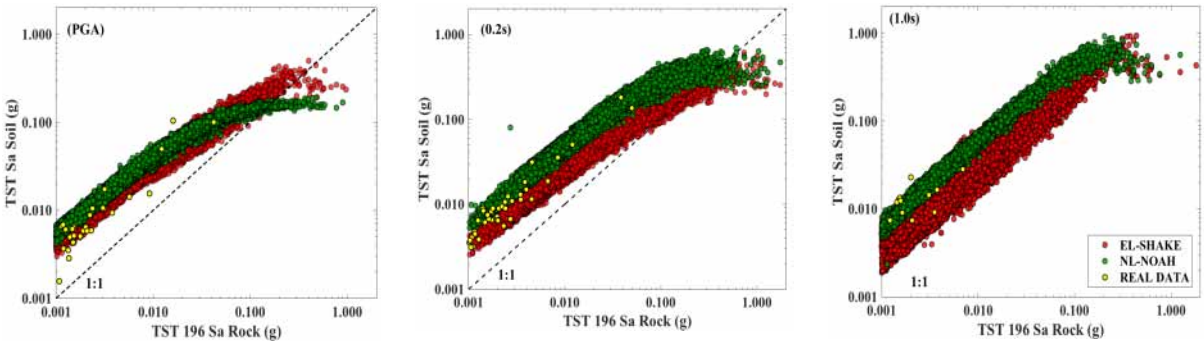

Figure 7. Equivalent linear (SHAKE91, red) and non-linear (NOAH, green) amplification factors compared with real data (yellow) for three different spectral periods (PGA, 0.2s and 1.0s).

To calibrate and validate our models, we compared the synthetic time histories on soil with current available data on site. **Figure 7** displays the plot relating the spectral acceleration on hard rock at the bottom of the Euroseistest basin, *TST196 Sa Rock (g)*, to the acceleration on soil at the surface, TST *Sa Soil (g)*, for the three considered different spectral periods and both EL (SHAKE91) and NL (NOAH) site response codes, together with the registered acceleration values from different events reported at the Euroseistest database (Pitilakis et al. 2013). The same amount of earthquakes were used at the three different spectral periods, nevertheless, only accelerations above 0.001g are displayed on this plot, this is the reason why the number of points varies from plot to plot. From visual inspection, it

is possible to say that the two models (EL and NL) are consistent with the actual Euroseistest site observations, and we can expect that the real median of the site is contained between the two proposed hazard models, since most of the data is located within the scatter of the two models and follows similar shape. One could possibly argue that SHAKE91 performs slightly better for low ground-motion levels [Sa < 0.01g], while NOAH might be preferable for intermediate ground-motion levels [0.01g ≤ Sa ≤ 0.1g]; no conclusion however can be drawn as to which model performs better for high acceleration level [Sa > 0.1], since there are no strong motion recordings. Related to the real data variability, it seems that the synthetic time histories and site response computations of both models (SHAKE and NOAH) slightly underestimate the actual variability, since some of the yellow points are located outside the scatter range of both cases (red and green dots in **Figure 7**).

6 CONCLUSIONS

We found relatively satisfactory consistency between both fully probabilistic methods (AM and SM) using the two different EL-SHAKE91 and NL-NOAH site response codes along all the studied periods. On this example case study, the code-to-code variability (SHAKE91 and NOAH) is found to control the uncertainty in terms of hazard estimates, rather than the method-to-method variability (AM and SM). It must be mentioned however that the numerical limitation of the AM approach for strongly non-linear sites, already acknowledged by its authors, prevents from retrieving the site surface hazard curve for intermediate and long return periods at the Euroseistest because of the ground motion saturation. The SM does not present this numerical limitation, and the hazard curve on soil was derived even at long return periods, yet, with a much higher computational price.

By comparing the two models with real in-situ data, we observed that the two site response models (EL and NL) are consistent with the site recordings, in terms both of median values and event-to-event variability. One can thus expect that the real median hazard estimate of the site will be contained between the two proposed hazard models, since most of the in-situ data are located within their dispersions. SHAKE91 may be thought to perform slightly better for low ground-motion levels [Sa soil < 0.01g], while NOAH would be preferable for intermediate ground-motion levels [0.01g ≤ Sa ≤ 0.1g]. No conclusion can be made at high acceleration level [Sa > 0.1] since no real data is available to calibrate the model on this range. We encourage the use of synthetic simulations calibrated wit real data such as the one we proposed in this paper, since it allows a better understanding and accounting of the variability of the physical phenomena, an improved parameterization of the input values, and a more robust probabilistic analysis. In most cases, this is presently not possible with real data because of their scarcity at high acceleration levels.

7 ACKNOWLEDGMENTS

This work has been supported by a grant from Labex OSUG@2020 (Investissements d'avenir – ANR10 LABX56 - http://www.osug.fr/labex-osug-2020/). Special thanks are due to Fabian Bonilla for providing his non-linear code NOAH and additional technical assistance on its usage. We thank Fabrice Hollender for providing valuable geotechnical and site-specific data to build the non-linear models. All ground-motion synthetics used in this study were generated using Boore 2003 Stochastic Method and his open source code SMSIM (http://www.daveboore.com/). Hazard calculations on rock have been performed using the Openquake engine and the post-processing toolkits developed by the GEM Foundation (http://www.globalquakemodel.org/), as well as the SHARE area source model (http://www.share-eu.org/).

8 REFERENCES

Akkar, S., Sandıkkaya, M. A., Bommer, J. J. (2014). Empirical ground-motion models for point-and extended-source crustal earthquake scenarios in Europe and the Middle East. Bulletin of Earthquake Engineering, 12(1), 359-387.

Al Atik L, Kottke A, Abrahamson N, Hollenback J (2014) ost vibration theory approach. Bull Seismol Soc Am 104(1):336–346.

Aristizábal C., Bard P.Y., Beauval C. (2018a). Site-Specific PSHA: Combined Effects of Single-Station-Sigma, Host-to-Target Adjustments and Nonlinear Behavior. Bulletin of Earthquake Engineering (In preparation).

Aristizábal C., Bard P.Y., Gómez J.C., Beauval C. (2018b). Integration of Site Effects into PSHA: A Comparison Between Two Fully Probabilistic Methods on the Euroseistest.. Geosciences (Switzerland) (In prepaation).

Aristizábal, C., P-Y. Bard and C. Beauval, (2017). Site-specific PSHA: Combined effects of single station sigma, host-to-target adjustments and non-linear behavior. 16WCEE 2017 (16th World Conference on Earthquake Engineering, Santiago Chile, January 9-13, 2017), paper # 1504, 12 pages.

Bazzurro, P., Cornell, C. A. (2004a). Ground-motion amplification in nonlinear soil sites with uncertain properties. Bulletin of the Seismological Society of America, 94(6), 2090-2109.

Bazzurro, P., Cornell, C. A. (2004b). Nonlinear soil-site effects in probabilistic seismic-hazard analysis. Bulletin of the Seismological Society of America, 94(6), 2110-2123.

Biro, Y., Renault, P. (2012, September). Importance and impact of host-to-target conversions for ground motion prediction equations in PSHA. In Proc. of the 15th World Conference on Earthquake Engineering (pp. 24-28).

Bonilla, L. F. (2001). NOAH: users manual. Institute for Crustal Studies, University of California, Santa Barbara.

Boore, D. M. (2003). Simulation of ground motion using the stochastic method. In Seismic Motion, Lithospheric Structures, Earthquake and Volcanic Sources: The Keiiti Aki Volume (pp. 635-676). Birkhäuser Basel.

Boore, D. M. (2003). Simulation of ground motion using the stochastic method. In Seismic Motion, Lithospheric Structures, Earthquake and Volcanic Sources: The Keiiti Aki Volume (pp. 635-676). Birkhäuser Basel.

Boore, D. M. (2005). SMSIM: Fortran programs for simulating ground motions from earthquakes: Version 2.3. US Department of the Interior, US Geological Survey.

Boore, D. M. (2005). SMSIM: Fortran programs for simulating ground motions from earthquakes: Version 2.3. US Department of the Interior, US Geological Survey.

Campbell KW (2003) Prediction of strong ground motion using the hybrid empirical method and its use in the development of ground-motion (attenuation) relations in eastern North America. Bull Seismol Soc Am 93(3):1012–1033

Carver, D., Bollinger, G. A. (1981). Aftershocks of the June 20, 1978, Greece earthquake: a multimode faulting sequence. Tectonophysics, 73(4), 343-363.

Chávez-Garcıa, F. J., Raptakis, D., Makra, K., & Pitilakis, K. (2000). Site effects at Euroseistest—II. Results from 2D numerical modeling and comparison with observations. Soil Dynamics and Earthquake Engineering, 19(1), 23-39.

Cotton, F., Scherbaum, F., Bommer, J. J., Bungum, H. (2006). Criteria for selecting and adjusting ground-motion models for specific target regions: Application to central Europe and rock sites. Journal of Seismology, 10(2), 137-156.

Delavaud, E., Scherbaum, F., Kuehn, N., Allen, T. (2012). Testing the global applicability of ground-motion prediction equations for active shallow crustal regions. Bulletin of the Seismological Society of America, 102(2), 707-721.

Idriss, I. M., Sun, J. I. (1993). User's manual for SHAKE91: a computer program for conducting equivalent linear seismic response analyses of horizontally layered soil deposits. Center for Geotechnical Modeling, Department of Civil and Environmental Engineering, University of California, Davis.

Jongmans, D., Pitilakis, K., Demanet, D., Raptakis, D., Riepl, J., Horrent, C., ... & Bard, P. Y. (1998). EURO-SEISTEST: Determination of the geological structure of the Volvi basin and validation of the basin response. Bulletin of the Seismological Society of America, 88(2), 473-487.

Kottke AR (2017) VS30–k0 relationship implied by ground motion models? In: 16WCEE 2017 (16th world conference on earthquake engineering, Santiago, Chile, January 9–13, 2017), paper # 3089.

Ktenidou OJ, Abrahamson NA (2016) Empirical estimation of high-frequency ground motion on hard rock. Seismol Res Lett 87(6):1465–1478.

Ktenidou OJ, Abrahamson NA, Drouet S, Cotton F (2015) Understanding the physics of kappa (κ): insights from a downhole array. Geophys J Int 203(1):678–691

Laurendeau, A., Bard, P. Y., Hollender, F., Perron, V., Foundotos, L., Ktenidou, O. J., & Hernandez, B. (2017). Derivation of consistent hard rock (1000 < VS < 3000 m/s) GMPEs from surface and down-hole recordings: analysis of KiK-net data. Bulletin of Earthquake Engineering, 32 pages, open access publication, DOI 10.1007/s10518-017-0142-6

Liotier, Y. (1989). Modelisation des ondes de volume des seismes de l'arc Ageen. DEA de l'Universite Joseph Fourier, Grenoble, France.

Manakou, M. V., Raptakis, D. G., Chávez-García, F. J., Apostolidis, P. I., Pitilakis, K. D. (2010). 3D soil structure of the Mygdonian basin for site response analysis. Soil Dynamics and Earthquake Engineering, 30(11), 1198-1211.

Maufroy E, Chaljub E, Hollender et al (2015). Earthquake ground-motion in the Mygdonian basin, Greece: the E2VP verification and validation of 3D numerical simulation up to 4 Hz. Bulletin of the Seismological Society of America, v. 105, p. 1398-1418, doi:10.1785/0120140228.

Maufroy E, Chaljub E, Hollender F (2016). Numerical simulation and ground-motion prediction: Verification, validation and beyond - lessons from the E2VP project. Soil Dynamics & Earthquake Engineering (0267-7261), December 2016, Vol. 91, p53-71. 19p. DOI: 10.1016/j.soildyn.2016.09.047.

Maufroy E, Chaljub E, Theodoulidis N et al (2017). Source-related variability of site response in the Mygdonian Basin (Greece) from accelerometric recordings and 3D numerical simulations. Bulletin of the Seismological Society of America, January 17, 2017, Vol. Pre-Issue Publication DOI: 10.1785/0120160107.

Pagani, M., Monelli, D., Weatherill, G., Danciu, L., Crowley, H., Silva, V., ... & Simionato, M. (2014). OpenQuake engine: an open hazard (and risk) software for the global earthquake model. Seismological Research Letters, 85(3), 692-702.

Papaspiliou, M., Kontoe, S., Bommer, J. J. (2012a). An exploration of incorporating site response into PSHA—Part I: Issues related to site response analysis methods. Soil Dynamics and Earthquake Engineering, 42, 302-315.

Papaspiliou, M., Kontoe, S., Bommer, J. J. (2012b). An exploration of incorporating site response into PSHA-part II: Sensitivity of hazard estimates to site response approaches. Soil Dynamics and Earthquake Engineering, 42, 316-330.

Pitilakis, K., D. Raptakis, K. Lontzetidis, Th. Tika-Vassilikou, and D. Jongmans, 1999. Geotechnical And Geophysical Description Of Euro-Seistest, Using Field, Laboratory Tests And Moderate Strong Motion Recordings. Journal of Earthquake Engineering 1999 03:03, 381-409

Pitilakis, K., Roumelioti, Z., Raptakis, D., Manakou, M., Liakakis, K., Anastasiadis, A., & Pitilakis, D. (2013). The EUROSEISTEST Strong-Motion Database and Web Portal. Seismological Research Letters, 84(5), 796-804.

Raptakis, D., Chávez-Garcıa, F. J., Makra, K., & Pitilakis, K. (2000). Site effects at Euroseistest—I. Determination of the valley structure and confrontation of observations with 1D analysis. Soil Dynamics and Earthquake Engineering, 19(1), 1-22.

Raptakis, D., Theodulidis, N., & Pitilakis, K. (1998). Data analysis of the Euroseistest strong motion array in Volvi (Greece): Standard and horizontal-to-vertical spectral ratio techniques. Earthquake Spectra, 14(1), 203-224.

Riepl, J., Bard, P. Y., Hatzfeld, D., Papaioannou, C., & Nechtschein, S. (1998). Detailed evaluation of site-response estimation methods across and along the sedimentary valley of Volvi (EURO-SEISTEST). Bulletin of the Seismological Society of America, 88(2), 488-502.

Schnabel, P. B. (1972). SHAKE a computer program for earthquake response analysis of horizontally layered sites. EERC Report, Univ. of California, Berkeley.

Schnabel, P. B., Lysmer, J., Seed, H. B (1992). SHAKE-91: equivalent linear seismic response analysis of horizontally layered soil deposits, the earthquake engineering online archive NISEE e-library.

Van Houtte, C., Drouet, S., Cotton, F. (2011). Analysis of the origins of κ (kappa) to compute hard rock to rock adjustment factors for GMPEs. Bulletin of the Seismological Society of America, 101(6), 2926-2941.

Woessner, J., Laurentiu, D., Giardini, D., Crowley, H., Cotton, F., Grünthal, G., ... & Hiemer, S. (2015). The 2013 European seismic hazard model: key components and results. Bulletin of Earthquake Engineering, 13(12), 3553-3596.